RSC Advances

PAPER

View Article Online
View Journal | View Issue

Cite this: *RSC Adv.*, 2021, **11**, 16142

The effect of 2D tungsten disulfide nanoparticles on Lewis lung carcinoma cells *in vitro*†

D. L. Kolesnik,[a] O. N. Pyaskovskaya,[a] O. P. Gnatyuk,[*b] V. V. Cherepanov,[b] S. O. Karakhim,[c] I. O. Polovii,[b] O. Yu. Posudievsky,[d] N. V. Konoshchuk,[d] V. V. Strelchuk,[e] A. S. Nikolenko,[e] G. I. Dovbeshko[b] and G. I. Solyanik[a]

The unique physicochemical properties of modern two-dimensional (2D) nanomaterials with graphene-like structures make them promising candidates for biology and medicine purposes. In this article, we investigate the influence of the two-dimensional tungsten disulfide (2D WS_2) water suspension nanoparticles obtained by an improved mechanochemical method from powdered WS_2 on morphological and structural characteristics of Lewis lung carcinoma cells using FT-IR, Raman spectroscopy, and confocal microscopy. The characterization of the 2D WS_2 nanoparticles by different physical methods is given also. We have highlighted that 2D WS_2 does not exert cytotoxic activity in the case of 1 day incubation with tumor cells. Prolongation of the incubation period up to 2 days has caused a statistically significant ($p < 0.05$) concentration-dependent decrease of the number of viable cells by more than 30% with the maximum cytotoxic effect at concentrations of 2D WS_2 close to 2 μg ml^{-1}. In the Raman spectra of 2D WS_2 treated cells the bands centered at 354 cm^{-1} and 419 cm^{-1}, which are assigned to characteristics and modes of WS_2 nanoparticles were observed. The obtained data indicate, that the cytotoxic effect of 2D WS_2 on tumor cells in the case of long-term incubation is realized particularly through the ability of 2D WS_2 to enter tumor cells and/or accumulate on their surface, which gives a rationale to conduct further studies of their antitumor efficacy *in vitro* and *in vivo* when combined with chemotherapeutic drugs.

Received 23rd February 2021
Accepted 9th April 2021

DOI: 10.1039/d1ra01469b

rsc.li/rsc-advances

Introduction

Modern graphene-like nanomaterials have many extraordinary physical and chemical properties, which makes them promising for solving various tasks in the fields of materials science, electronics, biology, medicine, *etc.*[1–6] 2D materials can be produced as dispersions, which expands their potential applications to obtain coatings, nanocomposites, heterostructures, and for biomedical application also.

2D nanomaterials are two-dimensional crystals with a very small thickness, which can be several atom layers. Transition metal dichalcogenides such as (MoS_2, WS_2, $MoSe_2$, $MoTe_2$, *etc.*) can form 2D materials due to their layered structure. Covalent bonds within a layer are much stronger than van der Waals's interaction between layers. Bulk materials WS_2 are semiconductors with an indirect band gap of approximately 1 eV, which becomes a direct bandgap of 1.8–2 eV upon the formation of nanosheets.[7,8] It is accompanied by the appearance of luminescence, which is absent in the bulk material. The maximum luminescence significantly depends on the size distribution of the layers.

In biomedical practice, such 2D nanomaterials could be useful for the diagnosis and treatment of various pathological conditions, including cancer. The use of 2D nanomaterials for diagnosis may include fluorescence, MRT, CT, and photoacoustic imaging of the pathological process. Therapeutic applications of those nanoparticles can be focused on photothermal and photodynamic therapy, chemotherapy as well as synergistic therapy.

Nowadays there are data on high prospects for the use of 2D MoS_2 and WS_2 nanomaterials as a drug delivery carrier. Despite the success in the development of a drug delivery system using graphene-like nanomaterials, the big challenge is their toxicity to normal organs and tissues.[9,10] Therefore, transition metal dichalcogenides (TMD) including molybdenum disulfide (MoS_2) and tungsten disulfide (WS_2) nanoparticles due to their

[a]*R. E. Kavetsky Institute of Experimental Pathology, Oncology and Radiobiology, National Academy of Sciences of Ukraine, 45 Vasylkivska str., Kyiv, 03022, Ukraine*
[b]*Department of Physics of Biological Systems, Institute of Physics of the National Academy of Sciences of Ukraine, Prospekt Nauki 46, Kyiv 03028, Ukraine. E-mail: hrysantemka@gmail.com*
[c]*Palladin Institute of Biochemistry of the National Academy of Sciences of Ukraine, Leontovicha Street 9, Kyiv 01601, Ukraine*
[d]*L. V. Pisarzhevsky Institute of Physical Chemistry of the National Academy of Sciences of Ukraine, Prospekt Nauki 31, Kyiv 03028, Ukraine*
[e]*V. E. Lashkaryev Institute of Semiconductor Physics of the National Academy of Sciences of Ukraine, Prospekt Nauki 41, Kyiv 03028, Ukraine*

† Electronic supplementary information (ESI) available. See DOI: 10.1039/d1ra01469b

layered structure and capability to be successfully loaded with anticancer drugs, have attracted considerable attention in recent years.[11–13] An additional advantage of inorganic graphene-like 2D nanomaterials is their low toxicity to normal organs and tissues.[14,15] In particular, an extremely high loading capacity of PEGylated 2D MoS_2 has been shown for the anticancer drug doxorubicin.[16] 2D WS_2 nanoparticles have been also reported to possess a high loading capacity for chemotherapeutic drugs, as confirmed by Yong *et al.* with methylene blue as a photosensitizer.[17] It has been shown that improvement in the therapeutic properties of WS_2 nanomaterials can be achieved by the fabrication of nanosheet-based nanocapsules with the inclusion of polyvinylpyrrolidone and iron(III).[18] The whole new level for delivery of chemotherapeutic drugs to the tumor was opened with the development of hybrid nanomaterials based on WS_2 nanosheets and liposomes, which significantly increases their adsorption and drug delivery capacities.[19]

For oncological applications, such properties as a large surface area of 2D WS_2 nanoparticles enable for creation of a directed drug delivery system. Nanoparticle-based drug delivery systems are aimed at improving in delivering the chemotherapeutic drugs into the tumor, impaired due to aberrant tumor angiogenesis[20,21] and, as a consequence, increasing the effectiveness of anticancer therapy.

It has been shown also that WS_2 in the form of quantum dots 1–1.5 nm in size can cause dissociation of hydrogen peroxide and exhibit catalytic properties in substrate oxidation through interaction with hydrogen peroxide (similar to natural peroxidases). Such peroxidase-like properties make WS_2 a promising material for biotechnology. The WS_2 nanoparticles themselves exhibit characteristic photoluminescence (PL) in the blue spectral region. The position of the luminescence maximum depends on the excitation wavelength and can appear in the range of 400–440 nm (*e.g.* at 420 nm under the excitation wavelength of 330 nm).[22] In the same work,[22] it was proposed to create a WS_2-based system for the determination of glucose levels by a proportional increase of the luminescence intensity.

The work[23] has shown the ability of WS_2 nanoparticles smaller than 5 nm in size to neutralize reactive oxygen species and significantly increase the survival rate of cells after their treatment with ionizing radiation. The protective effect of WS_2 nanoparticles against the action of gamma radiation has been confirmed in experiments performed on mice. It is noted that the WS_2 nanoparticles are easily excreted by the kidneys within 1 day and do not cause any toxic effect within 30 days after treatment.

It is known that for the successful use of potential medicinal products in oncology, including the nanomaterials for drug delivery applications they should not stimulate the growth and metastasis of malignant tumors and should not reduce the activity of the chemotherapeutics. One of the first and obligatory stages in the study of such agents is the analysis of their action on the viability and proliferative potential of tumor cells.

Therefore, the main objective of the present study was to investigate the effect of 2D tungsten disulfide nanoparticles on the viability and molecular-structural characteristics of Lewis lung carcinoma cells *in vitro*. We used 2D WS_2, obtained by the improved mechanochemical method, having sizes as 10–200 nm with a particle's thickness of one or several atomic layers. Murine Lewis lung carcinoma cells were used as a tumor model, which makes it possible to further study *in vitro* and *in vivo* the antitumor efficacy of 2D WS_2 nanoparticles loaded with anticancer drugs.

Materials and methods

Experimental tumor models

A variant of Lewis lung carcinoma cells, LLC/R9, obtained *via* the multistage experimental progression of the parental strain (LLC) *in vivo* towards the development of cisplatin resistance, was used as a tumor cell model.[24] The cells were maintained *in vitro* in RPMI 1640 medium (Sigma, USA) with the addition of 10% fetal bovine serum (Sigma, USA) and 40 μg ml^{-1} gentamicin at 37 °C in humidified conditions with 5% CO_2.

Test agent 2D WS_2

Graphene-like 2D WS_2 materials obtained by an improved mechanochemical method from powdered WS_2 (99%, particle size < 2 μm, # 243639, Sigma-Aldrich) were used as the test agent.[25,26] Physicochemical properties of WS_2 nanoparticles and the method of their production were described in detail in.[25] TEM images were obtained using a PEM125K (Selmi) microscope operating at 100 kV, using dispersions deposited on a copper mesh coated with a carbon film (Fig. 1).

AFM characterization of WS_2 nanoparticles was performed on the "Solver Pro M" system (NT-MDT, Russia). Particles from methanol solution were deposited as a drop onto an atomically smooth mica surface (SPI supplies, V-1 grade). The measurements were carried out after complete evaporation of the solvent in the semicontact (tapping) mode using probes of the type CSG30 (NT-MDT, 0.6 N m^{-1}, 48 kHz). AFM data showed that the particles were located on the substrate isolated from each other. The height of most of the particles was 1–10 nm, which corresponds to the thickness of 1–10 atomic layers of WS_2. Based on the analysis of the Z-profiles of particles, we estimated their lateral sizes as ≤ 200 nm after filter application (Fig. 2).[27]

These data are well agreed with the result from zeta potential and particle size distribution measurement. We use the

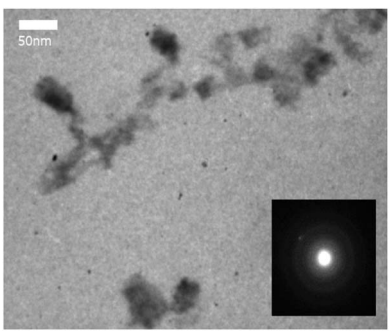

Fig. 1 TEM of WS_2 nanoparticles; SAED pattern (right lower corner).

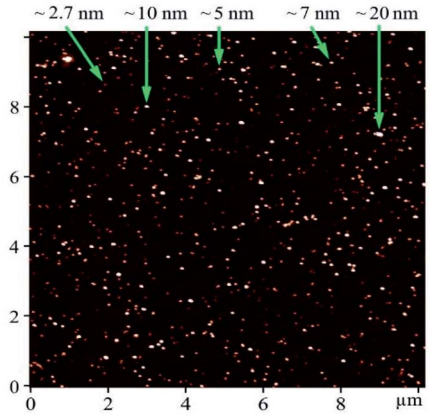

Fig. 2 AFM image of WS_2 particles deposited on mica substrate. Numbers with arrows show the height of objects.

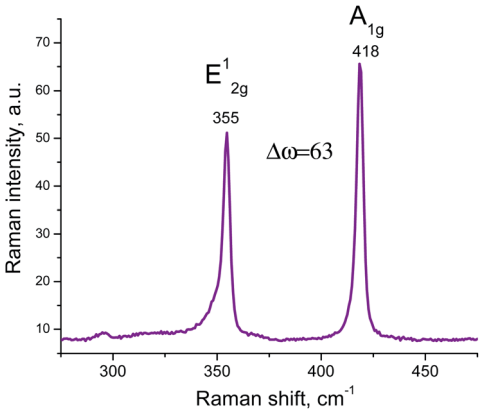

Fig. 4 Raman spectrum of the 2D WS_2 nanoparticles.

ZETASIZER Nano Series (Malvern, UK). The value of zeta potential is about −34.0 mV which means that our aqueous 2D WS_2 suspension is stable and not prone to aggregation (Fig. 3).

Raman spectra of 2D WS_2 show two characteristic bands in the region of 355 cm^{-1} and 418 cm^{-1}, related to E^1_{2g} and A_{1g} WS_2 vibrational modes respectively. In this study, an aqueous solution of nanostructured WS_2 at a concentration of 0.1 mg ml^{-1} (the maximum concentration at which the solution remained stable for a long time) was used. The differences between these two mode E^1_{2g} and A_{1g} corresponds to few layers 2D WS_2 nanoparticles (Fig. 4).

According to our previous studies, the pH of just obtained 2D WS_2 aqueous suspension may decreases about one point for one day, from 3.7 to 3.0. The nanoparticles oxidation processes in the aqueous medium may be a consequence of it. The oxidation occurs quickly for the first few days, and then the suspension remains stable up to 6–9 months. This should be taken into account when 2D WS_2 nanoparticles will be used as drug delivery systems in complexes with anticancer drugs.

Assessment of cytotoxicity of 2D WS_2 against LLC/R9

LLC/R9 cells were seeded in the wells of a 96-well plate at a density of 1.0 × 104 cells per well. After preincubation of the cells for 16–18 hours, the medium was replaced with a fresh one, which contained the test agent at the concentration of 0–25 μg ml^{-1}, and incubation continued for 1 or 2 days. Before adding into the medium 2D WS2 nanoparticles was filtered through polyethersulfone filter 0.2 micron (Sarstedt). Each concentration of the test agent was examined in triplicate. The cells incubated under the same conditions without treatment with the test agent were used as controls.

At the end of the incubation period, the cells were fixed in a cold 20% solution of trichloroacetic acid and stained with sulforhodamine B (Sigma, USA). The optical density of the test samples was evaluated using a plate reader Synergy HT (BioTek, USA) at a wavelength of 490 nm and used as an indicator of the number of viable LLC/R9 cells.

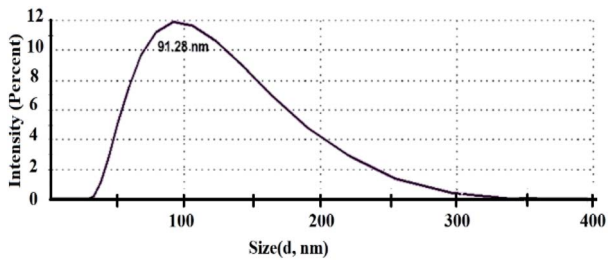

Fig. 3 Size distribution of 2D WS_2 nanoparticles.

Investigation of vibrational spectra of tumor cells

For spectroscopic studies (FT-IR absorption and Raman scattering), the samples of tumor cells were incubated for 2 days with WS_2 nanoparticles. LLC/R9 cells were seeded in 35 mm Petri dishes in the quantity of 0.2 million cells per dish. At the end of the pre-incubation period, the medium was replaced with the fresh one with the addition of WS_2 at a final concentration of 6 μg ml^{-1}, and the cells were incubated for 2 days. The cells incubated under the same conditions without the addition of WS_2 nanoparticles were used as control. After 2 days, the cells were mechanically removed from the plates, washed twice with PBS, pH 7.4, and resuspended in a small volume of H_2O. The resulting cell suspension was placed on a CaF_2 substrate transparent in the IR range and dried under a laminar air stream. The FT-IR spectra were registered with a Fourier IR spectrometer Bruker IFS-66 (Germany) in a wide spectral range from 3800 to 900 cm^{-1}. Assignment of the IR absorption bands to characteristic vibrations of the cells functional groups was done according to.[28–33] For all IR absorption spectra, the baseline correction and band intensity normalization by the Amide I band centered at 1651 cm^{-1} has been carried out.

Analysis of Raman spectra of tumor cells

Raman spectra were registered with a Raman spectrometer Horiba Jobin-Yvon T64000 (Germany) under a laser excitation wavelength of 488 nm and an excitation power of 100 mW. The samples of tumor cells treated and not treated with WS_2 nanoparticles were deposited on multilayer graphene

substrates. Baseline correction was performed for all spectra. No normalization of the spectra intensity was carried out.

Confocal images of tumor cell cultures

To obtained confocal images, LLC/R9 cells were seeded in 35 mm Petri dishes on rounded coverslips at a density of 0.2 million cells per dish and incubated overnight under standard conditions. At the end of the preincubation period, the medium was replaced with a fresh one with the addition of 2D WS_2 nanoparticles at a final concentration of 6 μg ml^{-1} and the incubation continued for 2 days. The cells incubated on coverslips under the same conditions without the addition of test nanoparticles were used as controls. Luminescence confocal images were obtained using a confocal laser scanning microscope Carl Zeiss LSM-510 META (Germany) with Plan-Neofluar 63x/0.75 Korr and 40x/0.6 Korr objectives. The fluorescence images were registered using Zeiss AxioCam digital camera. The PL excitation was carried out using a UV HBO 100 lamp with blue (FSet01 wf), green (Fset10 wf), or red (Fset20 wf) filters, or lasers with excitation wavelengths of 405 and 488 nm. For the fluorescence imaging, the tumor cells were left in the medium in the same Petri dishes, where they were cultured to maximize the preservation of viable cells. Parameters of confocal image registration were identical both for the control cells and those treated with WS_2 nanoparticles (Table 1).

Statistical analysis

Statistical processing of the obtained data was performed using descriptive statistics and non-parametric Mann–Whitney test using Microcal Origin and Statistica Software.

Results and discussion

Influence of WS_2 nanoparticles on the viability of LLC/R9 cells

Our study has shown that the effect of 2D WS_2 nanoparticles on the viability of Lewis lung cancer cells depends significantly on the concentration of this agent and the duration of its action. As can be seen in Fig. 5, under conditions of 1 day incubation, the test agent used in a wide range of concentrations has not caused a statistically significant decrease of the number of viable cells (compared to the corresponding control indices). This means that WS_2 nanoparticles incubated for 24 hours with tumor cells do not exert cytotoxic activity (*i.e.* do not cause tumor cell death during the incubation period) or cytostatic activity (do not inhibit the proliferation of these cells).

Prolongation of the incubation period of tumor cells with WS_2 nanoparticles up to 2 days has significantly changed their impact on the viability of tumor cells and has caused a statistically significant ($p < 0.05$) concentration-dependent decrease in the number of viable cells by more than 30% (Fig. 5).

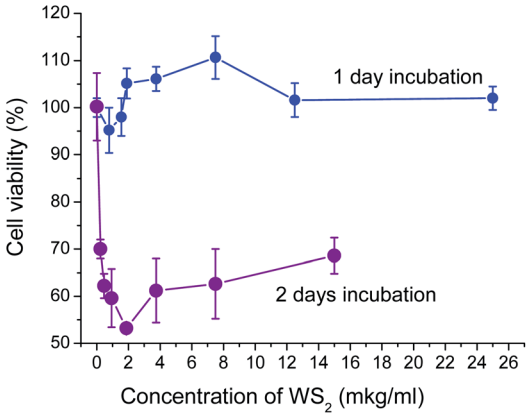

Fig. 5 Dependence of LLC/R9 cell viability on the concentration of 2D WS_2 nanomaterials in the culture medium under 1- and 2 days incubation.

The maximum cytotoxic/cytostatic effect of the WS_2 nanoparticles (the reduction of the number of viable cells by 47%) was recorded at concentrations close to 2 μg ml^{-1}. At the nanoparticle concentration higher than 2 μg ml^{-1}, their cytotoxic/cytostatic effect has not been enhanced: the number of viable cells remained at the level of 55–65% of that in the control. This pattern of the test agent's effect on the tumor cell viability may be related either to the heterogeneity of the tumor cell population (the presence of LLC/R9 cells sensitive and resistant to cytotoxic/cytostatic action of the nanoparticles) and/or to different mechanisms of nanoparticles effect on tumor cell viability (cytotoxic/cytostatic mechanisms along with mechanisms of stimulating effect on cell proliferation). A prolonged incubation period contributes to the cytotoxic/cytostatic impact more than the increase of the agent concentration. It is possible that the existence of two antagonistic mechanisms of the effect of nanoparticles on the viability of tumor cells is related to not only the tumor cell heterogeneity but the heterogeneous size distribution of the nanoparticles.

According to literature data, the authors underline low toxicity of the WS_2 and MoS_2 nanoparticles.[34] However different particles could influence by different manner as well a protocol of toxicity studying is different. In our case smaller in size nanoparticles can more easily be internalized by tumor cells and affect their viability, in particular, by reactive oxygen species neutralizing, as has been shown for WS_2 nanodots.[25]

Table 1 Parameters of confocal image registration

Scan Zoom	1.0
Objective	LD Plan-Neofluar 40x/0.6 Korr
Average	Line 8
Pinhole	Ch2: 808 mkm
Filters	Ch2-1: BP 505–570 IR; Ch 2-2: BP 420–480
Beam splitters	MBS: HFT 405/488/543/633; DBS1: mirror; DBS2: mirror; FW1: none
Wavelength	488 nm T1 50.0%, 405 nm T2 30.0%

Larger in size WS_2 nanoparticles can interact with macromolecules of tumor cells, such as DNA and proteins (especially membranotropic ones), causing either cell death or inhibiting their proliferative activity. Such an interaction can significantly affect the structure and/or concentration of the macromolecules in the cell, the change of which could be the most sensitively assessed by spectroscopic methods.

Therefore, to investigate the possible mechanisms of cytotoxic/cytostatic action of 2D WS_2 nanoparticles, the analysis of vibrational spectra (Raman scattering and IR absorption) of LLC/R9 cells after their 2 day incubation with nanoparticles at a concentration of 6 μg ml^{-1} (which reduces the number of viable cells approximately by 40%) has been performed.

Analysis of Raman spectra of tumor cells treated with WS_2 nanoparticles

The analysis of the Raman spectra of LLC/R9 cells has been performed after their 2 day incubation with WS_2 nanoparticles. A multilayer graphene substrate has been used for the spectra registration. Our previous studies[35–37] have shown good prospects of graphene as substrates for SERS Raman spectroscopy, as they are characterized by minimum luminescence and, in contrast to usual glass coverslip substrates, provide enhancement of vibrational bands intensity of the studied biological objects without changing their line shapes and frequency positions. The Raman spectra of LLC/R9 cells after their incubation with the investigated nanoparticles are presented in Fig. 6 a–c.

A detailed analysis of the Raman spectra has revealed the presence of characteristic Raman bands of the cells; the data with their assignments are presented in Table 2.[38]

In the Raman spectra of the cells treated with WS_2 nanoparticles, the bands centered at 354 cm^{-1} and 419 cm^{-1}, which are assigned to characteristic and modes of WS_2 nanoparticles,[39,40] are observed, that indicates the presence of test nanoparticles on the surface and/or inside the cells (Fig. 6 b and c). No other significant differences are observed between the spectra of cells treated and not treated with WS_2 nanoparticles, such as frequency shifts or band contour changes (Table 2).

Analysis of FT-IR spectroscopy data on the LLC/R9 cells after WS_2 treatment

In contrast to the Raman spectra, the analysis of the IR absorption spectra showed a pronounced effect of the WS_2 nanoparticles on the conformational state of the protein and nucleic acid fractions of the tumor cells.

In the region 1800–1500 cm^{-1}, the main contribution to the absorption is made by the total protein fraction (membrane proteins and proteins present in the cell). There are two clear absorption bands that refer to amide I (centered at 1650 cm^{-1}, stretching vibration C=O together with the deformation vibrations CN, NH) and amide II (centered at 1540 cm^{-1}, stretching vibrations CN, CHN, and deformation NH vibrations). The amide I band in our case has two shoulders 1651 cm^{-1} and 1630 cm^{-1}, which can be assigned to the α-helical structures and the β-sheet structures of the protein

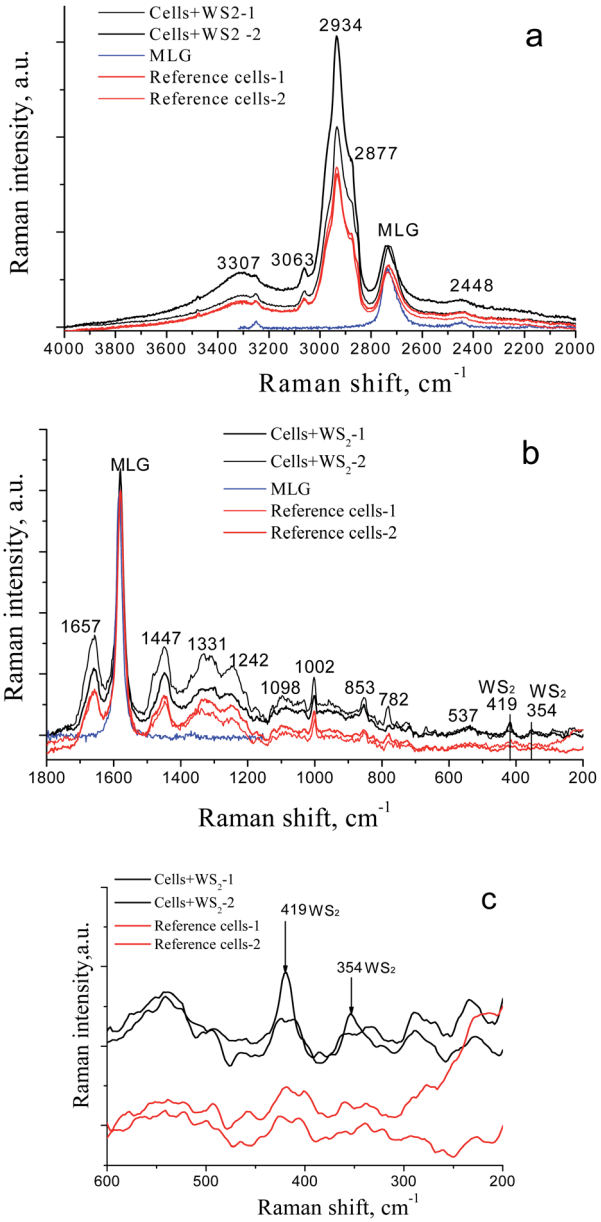

Fig. 6 Raman spectra of the LLC/R9 tumor cells in the different spectral regions, after (black curves, two spectra) and without treatment with 2D WS_2 nanoparticles (reference, red curves, two spectra). The blue curve is the Raman spectrum of the multilayer graphene (MLG) substrate. a – 4000–2000 cm^{-1}, b – 1800–200 cm^{-1}, c – 600–200 cm^{-1}.

fraction, respectively. After treatment of the cells with WS_2 nanoparticles, we registered the narrowing of the amide I band due to the reduction of contribution of the shoulder 1630 cm^{-1} (β-structures), which indicates conformational changes of proteins (Fig. 7).

The bands at 1454 cm^{-1} and 1395 cm^{-1} can be assigned to asymmetric and symmetric deformation vibrations of CH groups of proteins. Frequency shifts in this area were not observed, but one could note the decrease of the intensity of these bands in the cell samples after treatment with WS_2 nanoparticles.

Table 2 Major Raman bands of the LLC/R9 cells and their assignment to functional groups vibrations

Peak position, cm^{-1}	Assignment
3307	OH stretching vibrations
3063	CH ring of lipids
2934	CH_3 symmetric band of lipids and proteins
2877	CH_2 asymmetric stretch of lipids and proteins
2732	2D-mode, multilayer graphene
2448	
1657	Amide I (α-helix)
1580	G- mode, multilayer graphene
1447	CH_2 deformation
1331	CH_3 DNA & phospholipids
1242	Asymmetric phosphate [PO_2^- (*asym.*)] stretching modes
1098	C–C vibration mode
1002	Phenylalanine
853	(C–O–C) skeletal mode
782	Thymine, cytosine, uracil
537	Cholesterol ester
419	A_{1g} of WS_2
354	E^1_{2g} of WS_2

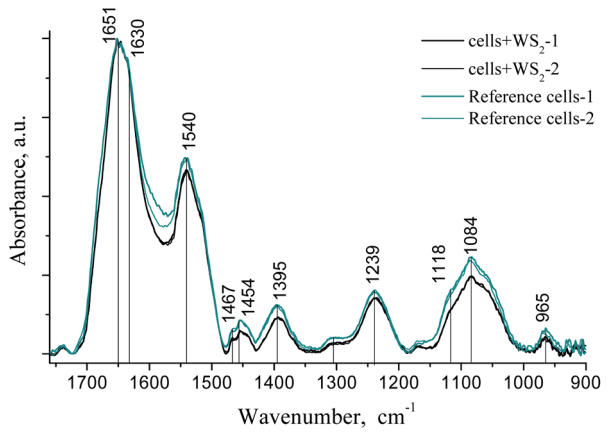

Fig. 7 FT-IR spectra of the LLC/R9 cells after 2D WS_2 treatment (two black lines) and without treatment (reference, two green lines).

In the range of 1350–1000 cm^{-1}, we also observed a decrease in the intensity and the half-width of the bands in the IR absorption spectra of the samples after WS_2 treatment. In this region, the main contribution to the absorption is made by PO_2^- groups of membrane phospholipids and the sugar phosphate backbone of nucleic acids (asymmetric 1239 cm^{-1} and symmetric 1084 cm^{-1} stretching vibrations).

Narrowing of the phosphate and amide bands after incubation with 2D WS_2 nanoparticles could be associated with the ordering of lipids and proteins near the particle surface. We observed the same effect by studying the formation of amyloid fibrils during the interaction of the nanoparticles with lysozyme at low pH.[41] No frequency shift of the main absorption bands was observed.[41]

Analysis of confocal images of tumor cells

Analysis of images obtained by confocal microscopy has shown that tumor cells treated with 2D WS_2 nanoparticles (Fig. 8a), do not differ significantly by their morphology from the control cells (Fig. 8b). In both cases, the vast majority of the cells were visually viable and remained spread on the glass; the cell population consisted of heterogeneous subpopulations of fibroblast-like and rounded cells, which is characteristic of this culture.

However, in the case of cells treated with 2D WS_2, the number of rounded cells was slightly more than in the control. Besides, the increase of the luminescence intensity from the cells incubated with nanoparticles in the blue region indicates that the particles either affect the biochemical processes in the cell or exert self-luminescence in the range of 380–480 nm. The latter statement is valid for very small particles (nanodots) 1–2 nm in size 15, the presence of which cannot be excluded in a heterogeneous mixture of particles with a size of tens of nm. Given their easier penetration into the cell due to their small size, it can be assumed that such small nanoparticles can penetrate into the cytoplasm of the cell and be localized around the cell nucleus, as evidenced by detailed image analysis. The luminescence of 2D WS_2 nanoparticles in the blue region has been observed by us earlier, but the study[42] showed the possibility of 2D WS_2 luminescence in the red region. The position of the luminescence band may depend on the size and structure of nanoparticles, as well as on the excitation wavelength.[23]

According to the study,[23] the WS_2 nanodots can catalyze some transformations involving charges, promoting electron transfer, eliminating oxidation products, and performing protective functions toward the DNA and cell nucleus; indeed, they are mainly located around the cell nuclei in our confocal images. However, based on our data, the opposite scenario could not be excluded, and then it may indicate the initial stages of 2D WS_2 induced cell death by apoptosis and/or necrosis, which may be one of the mechanisms of cytotoxic action of the studied nanoparticles and requires further research.

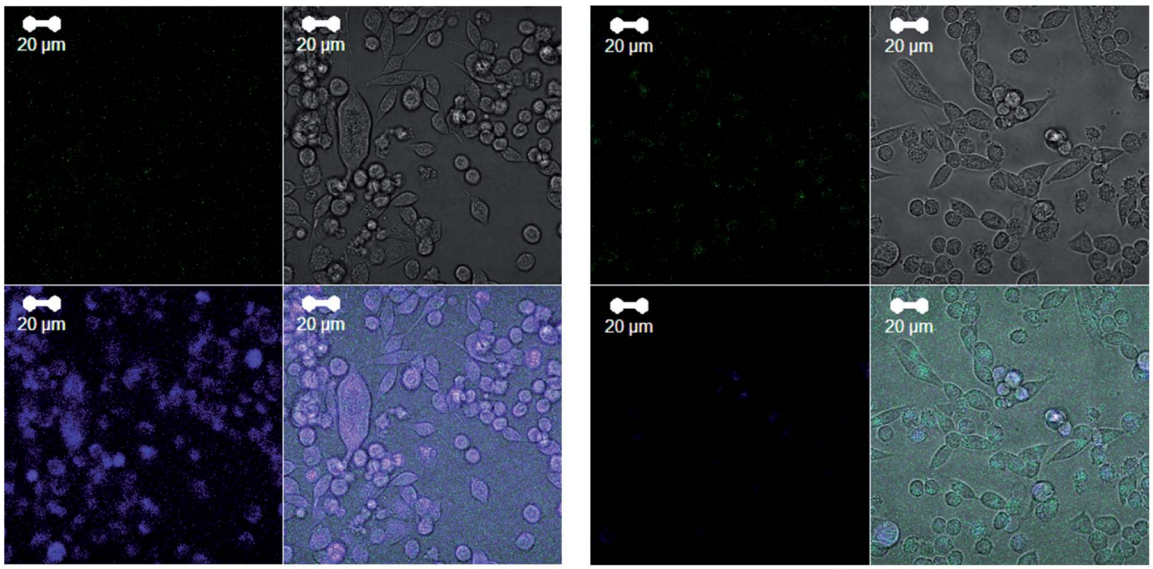

Fig. 8 Confocal microscopy images of LLC/R9 cells incubated for 2 days on glass coverslips: (a) with 2D WS_2 nanoparticles at a final concentration of 6 μg ml^{-1} and (b) without treatment, reference.

Therefore, our study has shown that 2D WS_2 nanoparticles in the conditions of short-term incubation did not significantly affect the viability of tumor cells, but showed a cytotoxic/cytostatic effect after the prolonged incubation period. The cytotoxic effect of the studied 2D nanomaterials was at least in part, due to their ability to enter tumor cells (and/or adsorb on their surface), which was confirmed by the presence of characteristic bands in the Raman spectra of the tumor cell samples. The ability of WS_2-based 2D nanomaterials not only to accumulate in tumor cells but also to show cytotoxic activity against tumor cells gives a rationale to conduct further research of their antitumor efficacy *in vitro* and *in vivo* when combined with chemotherapeutic drugs.

Conclusions

(1) 2D WS_2 nanoparticles aqueous suspension were obtained by an improved mechanochemical method from powdered WS_2. The height of particles was 1–10 nm, which corresponds to the thickness of 1–10 atomic layers of WS_2, and their lateral sizes was up to 200 nm. The suspension remains stable up to 6–9 months without any changes of properties or aggregation. But for the first few days the oxidation processes may occurs. This fact should be taken into account when 2D WS_2 nanoparticles will be used as drug delivery systems in complexes with anticancer drugs.

(2) It is established that WS_2-based 2D nanomaterials don't show cytotoxic and/or cytostatic effects on Lewis lung carcinoma cells under 1 day incubation and show concentration-dependent more than 30% decrease of the number of viable cells during a long-term incubation period up to 2 days. The last data indicate the process of oxidation in the cites of WS_2 particle's location and cell degradation.

(3) The analysis of Raman spectra of tumor cells treated with 2D WS_2 nanoparticles showed the presence of E^1_{2g} and A_{1g} modes of WS_2 indicating the ability of the nanoparticles to enter tumor cells and/or accumulate on their surface under their joint incubation *in vitro*.

(4) Multilayer graphene support was applied by us in Raman spectroscopy could be used as internal standard with good optical (strong reflectance, no fluorescence) and spectroscopic (accuracy of determination of wavenumber – 1580 cm^{-1} for ideal graphene layer) properties.

(5) The increased luminescence intensity of tumor cells incubated with 2D WS_2 nanoparticles in the blue spectral region makes it possible to further assert their passage into the cells, which can be used as a luminescence marker of 2D WS_2 activity.

(6) This study gives a possibility to develop a strategy for further loading the WS_2 nanoparticles with a drug in the tumor theranostics as well in other disease treatment (*e.g.* amiloid-like diseases).

Author contributions

D. L. Kolesnik – investigation, writing – original draft, work with cell culture, cell viability investigation and analysis. O. N. Pyaskovskaya – original draft, work with cell culture, cell viability investigation and analysis. O. P. Gnatyuk – investigation, writing – original draft, FTIR spectra registration and analysis. V. V. Cherepanov – investigation, TEM and AFM images registration and analysis. S. O. Karakhim – investigation, confocal images registration and analysis. I. O. Polovii – formal analysis. O. Yu. Posudievsky – resources, 2D WS_2 nanoparticles production. N. V. Konoshchuk – investigation, 2D WS_2 nanoparticles production, V. V. Strelchuk – investigation, Raman spectra registration and analysis. A. S. Nikolenko – investigation, Raman spectra registration and analysis. G. I.

Dovbeshko – data curation, project administration, writing – review & editing. G. I. Solyanik – data curation, writing – review & editing, supervision.

Conflicts of interest

There are no conflicts to declare.

Acknowledgements

This work was supported by the Ukrainian-Poland Project "Development of enhanced substrates based on 2D nanomaterials for fluorescent microscopy and spectroscopy", 2018–2019. Project "Development of 2D materials and "smart" sensors for medical and biological purposes" 11/1–2019, 2020 NATO SPS 985291 "A novel method for the detection of biohazards", 2017–2020. NRFU 2020.02/0027. We are thankful to Prof. V. A. Skryshevsky from the Taras Shevchenko National University of Kyiv, Faculty of Radiophysics, Electronics and Computer Systems for Zeta-potential measurement.

References

1 Z. Kou, X. Wang, R. Yuan, H. Chen, Q. Zhi, L. Gao, B. Wang, Z. Guo, X. Xue, W. Cao and L. Guo, *Nanoscale Res. Lett.*, 2014, **9**(1), 587, DOI: 10.1186/1556-276x-9-587.

2 P. T. Yin, S. Shah, M. Chhowalla and K.-B. Lee, *Chem. Rev.*, 2015, **115**(7), 2483, DOI: 10.1021/cr500537t.

3 Z. Fan, X. Huang, C. Tan and H. Zhang, *Chem. Sci.*, 2015, **6**, 95, DOI: 10.1039/c4sc02571g.

4 S. Ahmed and J. Yi, *Nano-Micro Lett.*, 2017, **9**, 50, DOI: 10.1007/s40820-017-0152-6.

5 W. Huang, Y. Sunami, H. Kimura and S. Zhang, *Nanomaterials*, 2018, **8**, 519, DOI: 10.3390/nano8070519.

6 L. Mei, S. Zhu, W. Yin, C. Chen, G. Nie, Z. Gu and Y. Zhao, *Theranostics*, 2020, **10**(2), 757, DOI: 10.7150/thno.39701.

7 T. P. Nguyen, W. Sohn, J. H. Oh, H. W. Jang and S. Y. Kim, *J. Phys. Chem. C*, 2016, **120**(18), 10078–10085, DOI: 10.1021/acs.jpcc.6b01838.

8 Y. Chen and M. Sun, *Nanoscale*, 2021, **13**(11), 5594–5619, DOI: 10.1039/d1nr00455g.

9 O. Akhavan, E. Ghaderi and A. Akhavan, *Biomaterials*, 2012, **33**(32), 8017–8025, DOI: 10.1016/j.biomaterials.2012.07.040.

10 K. P. Wen, Y. C. Chen, C. H. Chuang, H. Y. Chang, C. Y. Lee and N. H. Tai, *J. Appl. Toxicol.*, 2015, **35**(10), 1211–1218, DOI: 10.1002/jat.3187.

11 T. Liu, C. Wang, X. Gu, H. Gong, L. Cheng, X. Shi, L. Feng, B. Sun and Z. Liu, *Adv. Mater.*, 2014, **26**(21), 3433–3440, DOI: 10.1002/adma.201305256.

12 Y. Liu, J. Peng, S. Wang, M. Xu, M. Gao, T. Xia, J. Weng, A. Xu and S. Liu, *NPG Asia Mater.*, 2018, **10**, e458, DOI: 10.1038/am.2017.225.

13 V. Urbanová and M. Pumera, *Nanoscale*, 2019, **11**(34), 15770–15782, DOI: 10.1039/c9nr04658e.

14 J. Hao, G. Song, T. Liu, X. Yi, K. Yang, L. Cheng and Z. Liu, *Adv. Sci.*, 2017, **4**(1), 1600160, DOI: 10.1002/advs.201600160.

15 J. H. Appel, D. O. Li, J. D. Podlevsky, A. Debnath, A. A. Green, Q. H. Wang and J. Chae, *ACS Biomater. Sci. Eng.*, 2016, **2**(3), 361–367, DOI: 10.1021/acsbiomaterials.5b00467.

16 V. Yadav, S. Roy, P. Singh, Z. Khan and A. Jaiswal, *Small*, 2019, **15**, e1803706, DOI: 10.1002/smll.201803706.

17 Y. Yong, L. Zhou, Z. Gu, L. Yan, G. Tian, X. Zheng, X. Liu, X. Zhang, J. Shi, W. Cong, W. Yin and Y. Zhao, *Nanoscale*, 2014, **6**, 10394–10403.

18 C. Wu, S. Wang, J. Zhao, Y. Liu, Y. Zheng, Y. Luo, C. Ye, M. Huang and H. Chen, *Adv. Funct. Mater.*, 2019, **29**, 1901722, DOI: 10.1002/adfm.201901722.

19 Y. Liu and J. Liu, *Nanoscale*, 2017, **9**, 13187–13194, DOI: 10.1039/c7nr04199c.

20 S. Azzi, J. K. Hebda and J. Gavard, *Front. Oncol.*, 2013, **3**, 211, DOI: 10.3389/fonc.2013.00211.

21 R. Lugano, M. Ramachandran and A. Dimberg, *Cell. Mol. Life Sci.*, 2019, **77**, 1745, DOI: 10.1007/s00018-019-03351-7.

22 M. Haddad Irani-Nezhad, A. Khataee, J. Hassanzadeh and Y. Orooji, *Molecules*, 2019, **24**, 689, DOI: 10.3390/molecules24040689.

23 X. Bai, J. Wang, X. Mu, J. Yang, H. Liu, F. Xu, Y. Jing, L. Liu, X. Xue, H. Dai, Q. Liu, Y.-M. Sun, C. Liu and X.-D. Zhang, *ACS Biomater. Sci. Eng.*, 2017, **3**(3), 460, DOI: 10.1021/acsbiomaterials.6b00714.

24 G. I. Solyanik, A. G. Fedorchuk, O. N. Pyaskovskaya, O. I. Dasyukevitch, N. N. Khranovskaya, G. N. Aksenov and V. V. Sobetsky, *Exp. Oncol.*, 2004, **26**(4), 307.

25 O. Yu. Posudievsky, O. A. Khazieieva, A. S. Kondratyuk, V. V. Cherepanov, G. I. Dovbeshko, V. G. Koshechko and V. D. Pokhodenko, *Nanotechnology*, 2018, **29**, 085704, DOI: 10.1088/1361-6528/aaa381.

26 O. Yu. Posudievsky, O. A. Khazieieva, V. V. Cherepanov, G. I. Dovbeshko, A. G. Shkavro, V. G. Koshechko and V. D. Pokhodenko, *J. Mater. Chem. C*, 2013, **1**(39), 6411, DOI: 10.1039/c3tc30856a.

27 V. V. Cherepanov, A. G. Naumovets, O. Y. Posudievsky, V. G. Koshechko and V. D. Pokhodenko, *Nano Express*, 2020, **1**, 010004, DOI: 10.1088/2632-959x/ab763a.

28 Z. Movasaghi, S. Rehman and Dr I. ur Rehman, *Appl. Spectrosc. Rev.*, 2008, **43**(2), 134, DOI: 10.1080/05704920701829043.

29 G. I. Dovbeshko, N. Ya. Gridina, E. B. Kruglova and O. P. Pashchuk, *Talanta*, 2000, **53**(1), 233, DOI: 10.1016/s0039-9140(00)00462-8.

30 O. P. Repnytska, G. I. Dovbeshko, V. P. Tryndiak, I. M. Todor and D. V. Kosenkov, *Faraday Discuss.*, 2004, **126**, 61, DOI: 10.1039/b304904c.

31 G. Dovbeshko, V. Chegel, N. Gridina, O. Repnytska, Yu. Shirshov, V. Tryndiak, I. Todor and G. Solyanik, *Biopolymers*, 2002, **67**(6), 470, DOI: 10.1002/bip.10165.

32 O. P. Gnatyuk, G. I. Dovbeshko, A. Yershov, S. O. Karakhim, O. lchenko and O. Yu. Posudievsky, *RSC Adv.*, 2018, **8**, 30404, DOI: 10.1039/c8ra05085f.

33 K. Eberhardt, C. Matthaus, S. Marthandan, S. Diekmann and J. Popp, *PLoS One*, 2018, **13**(12), e0207380, DOI: 10.1371/journal.pone.0207380.

34 J. H. Appel, D. O. Li, J. D. Podlevsky, A. Debnath, A. A. Green, Q. H. Wang and J. Chae, *ACS Biomater. Sci. Eng.*, 2016, **2**(3), 361–367, DOI: 10.1021/acsbiomaterials.5b00467.

35 L. Dolgov, D. Pidgirnyi, G. Dovbeshko, T. Lebedieva, V. Kiisk, S. Heinsalu, S. Lange, R. Jaaniso and I. Sildos, *Nanoscale Res. Lett.*, 2016, **11**, 197, DOI: 10.1186/s11671-016-1418-5.

36 O. Fesenko, G. Dovbeshko, A. Dementjev, Re. Karpicz, T. Kaplas and Y. Svirko, *Nanoscale Res. Lett.*, 2015, **10**, 163, DOI: 10.1186/s11671-015-0869-4.

37 G. Dovbeshko, O. Gnatyuk, O. Fesenko, A. Rynder and O. Posudievsky, *J. Nanophotonics*, 2012, **6**(1), 061711, DOI: 10.1117/1.jnp.6.061711.

38 Z. Movasaghi, S. Rehman and Dr I. ur Rehman, *Appl. Spectrosc. Rev.*, 2007, **42**(5), 493, DOI: 10.1080/05704920701551530.

39 A. Berkdemir, H. Gutiérrez, A. Botello-Méndez, N. Perea-López, A. Elías, C.-I. Chia, B. Wang, V. Crespi, F. López-Urías, J.-C. Charlier, H. Terrones and M. Terrones, *Sci. Rep.*, 2013, **3**, 1755, DOI: 10.1038/srep01755.

40 X. Huang, Y. Gao, T. Yang, W. Ren, H.-M. Cheng and T. Lai, *Sci. Rep.*, 2016, **6**, 32236, DOI: 10.1038/srep32236.

41 I. O. Polovyi, O. P. Gnatyuk, K. O. Pyrshev, T. O. Hanulia, T. P. Doroshenko, S. A. Karakhim, O. Yu. Posudievsky, A. S. Kondratyuk, V. G. Koshechko and G. I. Dovbeshko, *Biochim. Biophys. Acta, Proteins Proteomics*, 2021, **1869**(1), 140556, DOI: 10.1016/j.bbapap.2020.140556.

42 X. H. Wang, J. Q. Ning, C. C. Zheng, B. R. Zhu, L. Xie, H. S. Wu and S. J. Xu, *J. Mater. Chem. C*, 2015, **3**, 2589, DOI: 10.1039/c5tc00016e.